

## Engineering Nonspherical Hollow Structures with Complex Interiors by Template-Engaged Redox Etching

Zhiyu Wang,<sup>†,§</sup> Deyan Luan,<sup>‡</sup> Chang Ming Li,<sup>†</sup> Fabing Su,<sup>#</sup> Srinivasan Madhavi,<sup>†,§</sup> Freddy Yin Chiang Boey,<sup>‡</sup> and Xiong Wen Lou<sup>\*†,§</sup>

*School of Chemical and Biomedical Engineering, Nanyang Technological University, 70 Nanyang Drive, Singapore 637457, School of Materials Science and Engineering, Nanyang Technological University, 50 Nanyang Avenue, Singapore 639798, Energy Research Institute at NTU, Nanyang Technological University, 50 Nanyang Drive, Singapore 637553, and State Key Laboratory of Multiphase Complex System, Institute of Process Engineering, Chinese Academy of Sciences, Beijing, China 100190*

Received September 10, 2010; E-mail: xwlou@ntu.edu.sg

**Abstract:** Despite the significant advancement in making hollow structures, one unsolved challenge in the field is how to engineer hollow structures with specific shapes, tunable compositions, and desirable interior structures. In particular, top-down engineering the interiors inside preformed hollow structures is still a daunting task. In this work, we demonstrate a facile approach for the preparation of a variety of uniform hollow structures, including  $\text{Cu}_2\text{O}@Fe(\text{OH})_x$  nanorattles and  $Fe(\text{OH})_x$  cages with various shapes and dimensions by template-engaged redox etching of shape-controlled  $\text{Cu}_2\text{O}$  crystals. The composition can be readily modulated at different structural levels to generate other interesting structures such as  $\text{Cu}_2\text{O}@Fe_2\text{O}_3$  and  $\text{Cu}@Fe_3\text{O}_4$  rattles, as well as  $Fe_2\text{O}_3$  and  $Fe_3\text{O}_4$  cages. More remarkably, this strategy enables top-down engineering the interiors of hollow structures as demonstrated by the fabrication of double-walled nanorattles and nanoboxes, and even box-in-box structures. In addition, this approach is also applied to form Au and  $\text{MnO}_x$  based hollow structures.

### Introduction

Hollow micro/nanostructures have been used in myriad applications such as photonic devices, energy storage, and microvessels for drug delivery and nanoscale reactors.<sup>1–10</sup> Common routes to fabricate hollow structures involve the growth of a shell of designed materials on various removable or sacrificial templates including hard templates such as mono-dispersed silica or polymer latex spheres and soft ones, for

example, emulsion micelles and even gas bubbles.<sup>11–22</sup> Templating methods are straightforward in concept but in practice often suffer from a main difficulty in coating desirable materials on template surface due to materials incompatibility issues. Several strategies have been employed for efficient coating based on different principles such as electrostatic interaction, chemical deposition, surface adsorption, and atomic layer deposition.<sup>13,20,23–29</sup> Methods based on other novel mechanisms like

<sup>†</sup> School of Chemical and Biomedical Engineering, Nanyang Technological University.

<sup>§</sup> Energy Research Institute at NTU, Nanyang Technological University.

<sup>‡</sup> School of Materials Science and Engineering, Nanyang Technological University.

<sup>#</sup> State Key Laboratory of Multiphase Complex System.

- (1) Lou, X. W.; Archer, L. A.; Yang, Z. C. *Adv. Mater.* **2008**, *20*, 3987.
- (2) Yin, Y. D.; Rioux, R. M.; Erdonmez, C. K.; Hughes, S.; Somorjai, G. A.; Alivisatos, A. P. *Science* **2004**, *304*, 711.
- (3) Lee, J.; Park, J. C.; Song, H. *Adv. Mater.* **2008**, *20*, 1523.
- (4) Zhu, Y. F.; Shi, J. L.; Shen, W. H.; Dong, X. P.; Feng, J. W.; Ruan, M. L.; Li, Y. S. *Angew. Chem., Int. Ed.* **2005**, *44*, 5083.
- (5) Li, J.; Zeng, H. C. *Angew. Chem., Int. Ed.* **2005**, *44*, 4342.
- (6) Hung, L.; Tsung, C. K.; Huang, W. Y.; Yang, P. D. *Adv. Mater.* **2010**, *22*, 1910.
- (7) Skrabalak, S. E.; Chen, J. Y.; Sun, Y. G.; Lu, X. M.; Au, L. S.; Copley, C. M.; Xia, Y. N. *Acc. Chem. Res.* **2008**, *41*, 1587.
- (8) Sun, Y. G.; Wiley, B.; Li, Z. Y.; Xia, Y. N. *J. Am. Chem. Soc.* **2004**, *126*, 9399.
- (9) Pang, M. L.; Hu, J. Y.; Zeng, H. C. *J. Am. Chem. Soc.* **2010**, *132*, 10771.
- (10) Cao, A. M.; Hu, J. S.; Liang, H. P.; Wan, L. J. *Angew. Chem., Int. Ed.* **2005**, *44*, 4391.

- (11) Zhong, Z. Y.; Yin, Y. D.; Gates, B.; Xia, Y. N. *Adv. Mater.* **2000**, *12*, 206.
- (12) Kim, S.; Kim, M.; Lee, W. Y.; Hyeon, T. *J. Am. Chem. Soc.* **2002**, *124*, 7642.
- (13) Caruso, F.; Caruso, R. A.; Mohwald, H. *Science* **1998**, *282*, 1111.
- (14) Yang, M.; Ma, J.; Zhang, C. L.; Yang, Z. Z.; Lu, Y. F. *Angew. Chem., Int. Ed.* **2005**, *44*, 6727.
- (15) Zoldesi, C. I.; Imhof, A. *Adv. Mater.* **2005**, *17*, 924.
- (16) Walsh, D.; Lebeau, B.; Mann, S. *Adv. Mater.* **1999**, *11*, 324.
- (17) Peng, Q.; Dong, Y. J.; Li, Y. D. *Angew. Chem., Int. Ed.* **2003**, *42*, 3027.
- (18) Dhas, N. A.; Suslick, K. S. *J. Am. Chem. Soc.* **2005**, *127*, 2368.
- (19) Lou, X. W.; Yuan, C. L.; Archer, L. A. *Small* **2007**, *3*, 261.
- (20) Yang, Z. Z.; Niu, Z. W.; Lu, Y. F.; Hu, Z. B.; Han, C. C. *Angew. Chem., Int. Ed.* **2003**, *42*, 1943.
- (21) Chen, M.; Wu, L.; Zhou, S.; You, B. *Adv. Mater.* **2006**, *18*, 801.
- (22) Lou, X. W.; Li, C. M.; Archer, L. A. *Adv. Mater.* **2009**, *21*, 2536.
- (23) Choi, W. S.; Koo, H. Y.; Kim, D. Y. *Adv. Mater.* **2007**, *19*, 451.
- (24) Sun, X. M.; Li, Y. D. *Angew. Chem., Int. Ed.* **2004**, *43*, 3827.
- (25) Caruso, F. *Adv. Mater.* **2001**, *13*, 11.
- (26) Zhou, J.; Liu, J.; Yang, R. S.; Lao, C. S.; Gao, P. X.; Tummala, R.; Xu, N. S.; Wang, Z. L. *Small* **2006**, *2*, 1344.
- (27) Fan, H. J.; Knez, M.; Scholz, R.; Nielsch, K.; Pippel, E.; Hesse, D.; Zacharias, M.; Gosele, U. *Nat. Mater.* **2006**, *5*, 627.
- (28) Wang, C. C.; Kei, C. C.; Yu, Y. W.; Peng, T. P. *Nano Lett.* **2007**, *7*, 1566.

galvanic replacement or Kirkendall effect have also been developed for more efficient production of hollow structures against sacrificial templates.<sup>2,7,8,30–33</sup> The fundamental driving force for creating hollow cavities is the difference between the shell material (or their precursor) and the template in physicochemical stability or reactivity.

The interior functionalization by encapsulating guest species has always been an important aspect of hollow structures. The incorporation of nano-objects as movable cores into hollow shells leads to the formation of rattle-like colloidal particles with multicomponent characteristics. The attraction of such structures is that multiple functions can be integrated into one structure for specific applications. The interactions between individual components also enable greatly improved overall performance or even new synergetic properties.<sup>8,34–36</sup> The most straightforward strategy for the synthesis of rattle-like structures is the so-called bottom-up approach, where the core and two concentric shells with different materials are constructed in an inner-to-outer order followed by selective removal of the inner shell by dissolution or annealing.<sup>8,23,36–42</sup> Strategies based on other mechanisms, such as inward diffusion, Kirkendall effect, inside-out Ostwald ripening, surfactant micelles templating, or partial dissolution of the cores, have also been reported recently.<sup>2,3,5,19,43–51</sup> However, the rattle-type structures obtained by bottom-up approaches are mostly spherical in morphology. Well-defined nonspherical nanorattles with tuneable core/shell compositions have been seldom fabricated due to difficulties ranging from forming uniform coating around high-curvature surfaces to the paucity of nonspherical templates available.

Hollow architectures with multilevel interiors represent a higher order of structuring and have spurred considerable interests very recently. The complex interior structures enable one to better control the local chemical microenvironment and multiple interface reactions for novel physicochemical properties such as the enhancement in photocatalytic activity, mechanical

strength, and preserved permeability.<sup>52–54</sup> A number of methods such as shell-by-shell templating or self-assembly of the nanoclusters have been successfully adopted to realize such unique hollow structures.<sup>8,19,34,37,14,55–58</sup> By forming alternating gold and silica shells on silica spheres from inner to outer, Halas and co-workers have first demonstrated the synthesis of nanospheres with multiple concentric shells of gold and silica.<sup>57</sup> We have recently demonstrated the synthesis of double-walled SnO<sub>2</sub>-based nanostructures by repeated hydrothermal deposition of SnO<sub>2</sub> against silica templates.<sup>19,37</sup> Soft-template methods also show their effectiveness for producing multiple-walled hollow spheres by surfactant-assisted assembly of tiny clusters despite of high specificity and scarcity in detailed mechanism for such systems.<sup>56,59–61</sup> In general, all these techniques belong to the category of bottom-up approaches. Construction of multilevel hollow structures by top-down approaches remains as a significant challenge until now.

In this work, we combine the redox reaction between Cu<sub>2</sub>O templates and Fe(III) ions with precisely controlled hydrolysis of iron ions to demonstrate one-step formation of hollow structures. Cu<sub>2</sub>O crystals are employed as sacrificial templates because of their diversity in crystal morphology, especially nonspherical shapes such as nanocubes, octahedra, and other highly symmetrical structures. They have been utilized as templates for the preparation of nonspherical mesocages of polyaniline (PANI) or Cu<sub>x</sub>S.<sup>62–64</sup> Note that insoluble Cu(I) oxide is a weak reducing agent; hollow structures would be created by redox etching of Cu<sub>2</sub>O to form soluble Cu(II) ions and simultaneous deposition of shell materials. It leads to the formation of a variety of interesting hollow structures such as nonspherical nanorattles of Cu<sub>2</sub>O@Fe(OH)<sub>x</sub> and hollow cages of Fe(OH)<sub>x</sub> depending on the reaction time. The chemical composition of these structures can be readily tuned by simple annealing to form a broad family of hollow structures such as nanorattles of Cu<sub>2</sub>O@Fe<sub>2</sub>O<sub>3</sub> and Cu@Fe<sub>3</sub>O<sub>4</sub>, as well as hollow cages of Fe<sub>2</sub>O<sub>3</sub> and Fe<sub>3</sub>O<sub>4</sub>. More remarkably, the approach presented here can be easily extended to top-down engineering the interiors of preformed hollow structures through repeated redox etching of the inner unreacted Cu<sub>2</sub>O cores. For example, double-walled cubic nanorattles and even box-in-box structures can be synthesized by template-engaged redox etching against Cu<sub>2</sub>O inside Fe(OH)<sub>x</sub> shells, which act as nanoscale reactors.

- (29) Zelikin, A. N.; Li, Q.; Caruso, F. *Angew. Chem., Int. Ed.* **2006**, *45*, 7743.  
 (30) Fan, H. J.; Gösele, U.; Zacharias, M. *Small* **2007**, *3*, 1660.  
 (31) Sun, Y. G.; Xia, Y. N. *Science* **2002**, *298*, 2176.  
 (32) Sun, Y. G.; Mayers, B. T.; Xia, Y. N. *Nano Lett.* **2002**, *2*, 481.  
 (33) Wang, Y. L.; Cai, L.; Xia, Y. N. *Adv. Mater.* **2005**, *17*, 473.  
 (34) Zeng, Y.; Wang, X.; Wang, H.; Dong, Y.; Ma, Y.; Yao, J. N. *Chem. Commun.* **2010**, *46*, 4312.  
 (35) Khalavka, Y.; Becker, J.; Sonnichsen, C. *J. Am. Chem. Soc.* **2009**, *131*, 1871.  
 (36) Kamata, K.; Lu, Y.; Xia, Y. N. *J. Am. Chem. Soc.* **2003**, *125*, 2384.  
 (37) Lou, X. W.; Yuan, C. L.; Archer, L. A. *Adv. Mater.* **2007**, *19*, 3328.  
 (38) Arnal, P. M.; Comotti, M.; Schüth, F. *Angew. Chem., Int. Ed.* **2006**, *45*, 8224.  
 (39) Liu, S. H.; Zhang, Z. H.; Han, M. Y. *Adv. Mater.* **2005**, *17*, 1862.  
 (40) Kim, M.; Sohn, K.; Na, H. B.; Hyeon, T. *Nano Lett.* **2002**, *2*, 1383.  
 (41) Lou, X. W.; Yuan, C. L.; Rhoades, E.; Zhang, Q.; Archer, L. A. *Adv. Funct. Mater.* **2006**, *16*, 1679.  
 (42) Lee, K. T.; Jung, Y. S.; Oh, S. M. *J. Am. Chem. Soc.* **2003**, *125*, 5652.  
 (43) Kim, S.; Yin, Y. D.; Alivisatos, A. P.; Somorjai, G. A.; Yates, J. T., Jr. *J. Am. Chem. Soc.* **2007**, *129*, 9510.  
 (44) Gao, J. H.; Liang, G. L.; Zhang, B.; Kuang, Y.; Zhang, X. X.; Xu, B. *J. Am. Chem. Soc.* **2007**, *129*, 1428.  
 (45) Lou, X. W.; Wang, Y.; Yuan, C. L.; Lee, J. Y.; Archer, L. A. *Adv. Mater.* **2006**, *18*, 2325.  
 (46) Peng, S.; Sun, S. H. *Angew. Chem., Int. Ed.* **2007**, *46*, 4155.  
 (47) Yang, H. G.; Zeng, H. C. *Angew. Chem., Int. Ed.* **2004**, *43*, 5206.  
 (48) Li, H. X.; Bian, Z. F.; Zhu, J.; Zhang, D. Q.; Li, G. S.; Huo, Y. N.; Li, H.; Lu, Y. F. *J. Am. Chem. Soc.* **2007**, *129*, 8406.  
 (49) Zeng, H. C. *Curr. Nanosci.* **2007**, *3*, 177.  
 (50) Liu, B.; Zeng, H. C. *Small* **2005**, *5*, 566.  
 (51) Liu, J.; Qiao, S. Z.; Hartono, S. B.; Lu, G. Q. *Angew. Chem., Int. Ed.* **2010**, *49*, 4981.

- (52) Zhao, Y.; Jiang, L. *Adv. Mater.* **2009**, *21*, 3621.  
 (53) Aizenberg, J.; Weaver, J. C.; Thanawala, M. S.; Sundar, V. C.; Morse, D. E.; Fratzl, P. *Science* **2005**, *309*, 275.  
 (54) Qian, J. F.; Liu, P.; Xiao, Y.; Jiang, Y.; Cao, Y. L.; Ai, X. P.; Yang, H. X. *Adv. Mater.* **2009**, *21*, 3663.  
 (55) Zhao, H.; Chen, J. F.; Zhao, Y.; Jiang, L.; Sun, J. W.; Yun, J. *Adv. Mater.* **2008**, *20*, 3682.  
 (56) Xu, H. L.; Wang, W. Z. *Angew. Chem., Int. Ed.* **2007**, *46*, 1489.  
 (57) Prodan, E.; Radloff, C.; Halas, N. J.; Nordlander, P. *Science* **2003**, *302*, 419.  
 (58) Pan, M. L.; Zeng, H. C. *Langmuir* **2010**, *26*, 5963.  
 (59) Wang, X. J.; Xu, D. S. *Adv. Mater.* **2010**, *22*, 1516.  
 (60) Zhang, L.; Qiao, S. Z.; Jin, Y. G.; Chen, Z. G.; Gu, H. C.; Lu, G. Q. *Adv. Mater.* **2008**, *20*, 805.  
 (61) Liu, J.; Hartono, S. B.; Jin, Y. G.; Li, Z.; Lu, G. Q.; Qiao, S. Z. *J. Mater. Chem.* **2010**, *20*, 4595.  
 (62) Zhang, Z. M.; Sui, J.; Zhang, L. J.; Wan, M. X.; Wei, Y.; Yu, L. M. *Adv. Mater.* **2005**, *17*, 2854.  
 (63) Jiao, S. H.; Xu, L. F.; Jiang, K.; Xu, D. S. *Adv. Mater.* **2006**, *18*, 1174.  
 (64) Cao, H. L.; Qian, X. F.; Wang, C.; Ma, X. D.; Yin, J.; Zhu, Z. K. *J. Am. Chem. Soc.* **2005**, *127*, 16024.

Furthermore, the versatility of this method is also demonstrated by the successful synthesis of Au and MnO<sub>x</sub> hollow structures.

## Experimental Section

**Synthesis of Cu<sub>2</sub>O Nanostructures.** Cu<sub>2</sub>O nanocubes with different sizes were synthesized by seed-mediated reaction with minor modification.<sup>65</sup> In our work, a mixture solution containing 0.2 M of sodium hydroxide (NaOH) and ascorbic acid was used to replace the solution of 0.2 M sodium ascorbate and the volume of all solutions was scaled up to 10 times. The Cu<sub>2</sub>O micro-octahedra were prepared by reducing copper sulfate with glucose in the presence of polyvinylpyrrolidone (PVP) in solution.<sup>66</sup> The Cu<sub>2</sub>O nanospheres were synthesized by the reaction between copper nitrate and hydrazine hydrate in 2-propanol in the presence of PVP.<sup>58</sup>

**Synthesis of Cu<sub>2</sub>O@Fe(OH)<sub>x</sub> Nanorattles and Fe(OH)<sub>x</sub> Nanocages.** The cubic nanorattles and nanoboxes were synthesized by dropwise adding 10 mL of ethanol solution of FeCl<sub>3</sub> (5.55 mM) into a suspension of 0.07 mmol of Cu<sub>2</sub>O nanocubes in 39 mL of the ethanol and 1 mL of NaCl solution (1.71 M) under stirring. Afterward, the products after different reaction times were collected by several rinse–centrifugation cycles and were dried in vacuum at 60 °C for further characterization. For the formation of octahedral rattles and cages, the same protocol was exploited except a higher concentration (92.5 mM) of the FeCl<sub>3</sub> solution was used. The hollow Fe(OH)<sub>x</sub> nanospheres were prepared following the same procedure for making cubic products while using 0.07 mmol of Cu<sub>2</sub>O nanospheres as templates.

**Synthesis of Cu<sub>2</sub>O@Fe<sub>2</sub>O<sub>3</sub> Nanorattles and Fe<sub>2</sub>O<sub>3</sub> Nanocages.** Cu<sub>2</sub>O@Fe<sub>2</sub>O<sub>3</sub> rattles and Fe<sub>2</sub>O<sub>3</sub> cages were made by annealing Cu<sub>2</sub>O@Fe(OH)<sub>x</sub> and Fe(OH)<sub>x</sub> products, respectively, at 250 °C in air for 3 h with a slow heating rate of 0.5 °C min<sup>-1</sup>. For both cubic and octahedral products, the annealing conditions were the same.

**Synthesis of Cu@Fe<sub>3</sub>O<sub>4</sub> and Fe<sub>3</sub>O<sub>4</sub> Nanocages.** Cu@Fe<sub>3</sub>O<sub>4</sub> rattles and Fe<sub>3</sub>O<sub>4</sub> cages were made by a similar process for making Fe<sub>2</sub>O<sub>3</sub>-based products except for annealing in a H<sub>2</sub>/N<sub>2</sub> flow. The annealing conditions are also the same for both cubic and octahedral products.

**Synthesis of Double-Walled Cu<sub>2</sub>O@Fe(OH)<sub>x</sub> Nanorattles and Fe(OH)<sub>x</sub> Nanoboxes.** The double-walled nanostructures were synthesized by repeating the preparation process for making single-walled products against Cu<sub>2</sub>O@Fe(OH)<sub>x</sub> nanorattles instead of the Cu<sub>2</sub>O nanocubes.

**Synthesis of Cu<sub>2</sub>O@Au Nanorattles, Au Nanoboxes, and Cu<sub>2</sub>O@MnO<sub>x</sub> Nanorattles.** The Cu<sub>2</sub>O@Au nanorattles and Au nanoboxes were synthesized by dropwise adding 10 mL of ethanol solution of HAuCl<sub>4</sub> (2 mM) into a suspension of 0.035 mmol of Cu<sub>2</sub>O nanocubes in 40 mL of ethanol and 2.5–5 mL of NaCl solution (1.71 M) under stirring. The Cu<sub>2</sub>O@MnO<sub>x</sub> nanorattles were synthesized by dropwise adding 0.4 mL of mixed aqueous solution of KMnO<sub>4</sub> (0.158 M) and hydrochloric acid (0.15 M) into a suspension of 0.035 mmol of Cu<sub>2</sub>O nanocubes in 20 mL of tertiary butanol and 1 mL of NaCl solution (1.71 M) under stirring. Afterward, the products after different reaction times were collected by several rinse–centrifugation cycles and were dried in vacuum at 60 °C for characterization.

**Material Characterization.** All samples were characterized by field-emission scanning electron microscope (FESEM, JEOL, JSM-6340F), transmission electron microscope (TEM, JEOL, JEM-2010), and X-ray diffraction (XRD, Bruker, D8-Advance X-ray Diffractometer, Cu Kα, λ = 1.5406 Å).

## Results and Discussion

Our strategy for synthesizing complex hollow structures is designed based on simultaneously coupled redox etching of

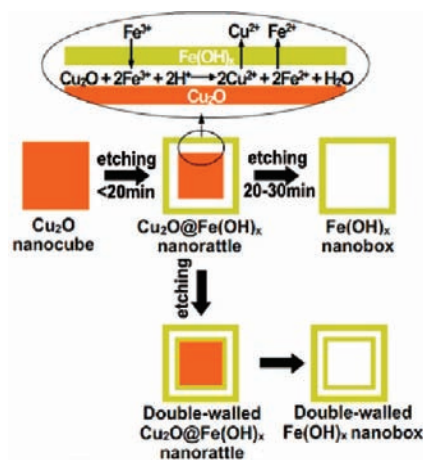
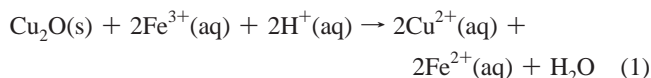


**Figure 1.** Schematic illustration of the formation of single-walled or double-walled hollow structures by template-engaged redox etching of Cu<sub>2</sub>O nanocubes.

Cu<sub>2</sub>O crystals and precisely controlled hydrolysis of iron ions, as schematically illustrated in Figure 1. Because the standard reduction potential of Fe<sup>3+</sup>/Fe<sup>2+</sup> pair (0.77 V, vs SHE) is higher than that of Cu<sup>2+</sup>/Cu<sub>2</sub>O (0.203 V, vs SHE), Cu<sub>2</sub>O crystals in suspension could be immediately oxidized by Fe(III) ions at room temperature according to the following redox reaction:<sup>67</sup>



The Fe(II) ions produced in this reaction are confined to the vicinity of template surface, where iron ions readily form hydroxides because of the depletion of H<sup>+</sup> ions by reaction 1, that is, increase of pH value locally. Once the concentration reaches a critical value, iron hydroxides (Fe(OH)<sub>x</sub>) can nucleate and grow into conformal shells around the scaffold of Cu<sub>2</sub>O templates. Simultaneously, a porous structure emerges within the shell as a result of outward flow of Cu(II) and Fe(II) ions and inward flow of Fe(III) ions while the Cu<sub>2</sub>O core is continuously consumed. As a result, a variety of nanostructures with tuneable hollow interiors such as nanorattles and nanoboxes can be synthesized, depending on the extent of reaction. During this process, the effect of acidic etching can be clearly ruled out because only white CuCl precipitate is formed rapidly when dilute HCl with estimated equivalent amount (15 μL, 37 wt %, calculated by assuming complete hydrolysis of FeCl<sub>3</sub>) is used to replace the FeCl<sub>3</sub>. In this regard, the mechanism involved in the present system is quite different from those based on simple acid-etching of metal oxide templates.<sup>68</sup>

The crystallographic structure and phase purity of the resultant hollow structures are examined by X-ray powder diffraction (XRD), as shown in Figure 2. The consumption of Cu<sub>2</sub>O templates upon etching is evidenced by remarkably decreased peak intensity as compared to that of initial Cu<sub>2</sub>O nanocubes. For the nanoboxes, signals from the Cu<sub>2</sub>O phase completely disappear to give a plane pattern without pronounced diffraction peaks. The iron hydroxide shells are amorphous in nature because the precipitation is carried out at room temperature.

(65) Kuo, C. H.; Chen, C. H.; Huang, M. H. *Adv. Funct. Mater.* **2007**, *17*, 3773.

(66) Sui, Y. M.; Fu, W. Y.; Yang, H. B.; Zeng, Y.; Zhang, Y. Y.; Zhao, Q.; Li, Y. E.; Zhou, X. M.; Leng, Y.; Li, M. H.; Zou, G. T. *Cryst. Growth Des.* **2010**, *10*, 99.

(67) Millazzo, G.; Caroli, S. *Tables of Standard Electrode Potentials*; John Wiley & Sons Inc.: New York, 1978.

(68) Liu, J. P.; Li, Y. Y.; Fan, H. J.; Zu, Z. H.; Jiang, J.; Ding, R. M.; Hu, Y. Y.; Huang, X. T. *Chem. Mater.* **2010**, *22*, 212.

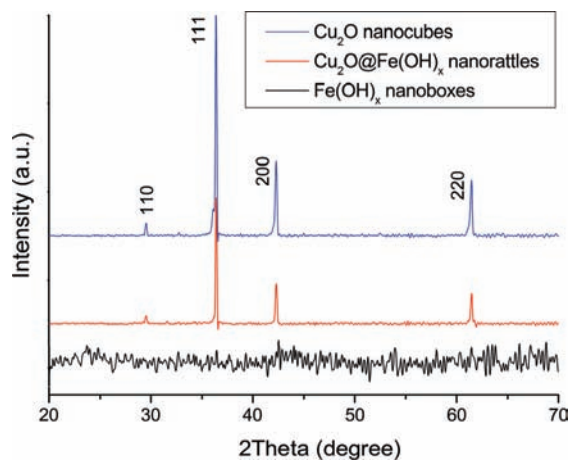


**Figure 2.** XRD patterns of  $\text{Cu}_2\text{O}$  nanocubes, cubic  $\text{Cu}_2\text{O}@Fe(\text{OH})_x$  nanorattles, and  $Fe(\text{OH})_x$  nanoboxes.

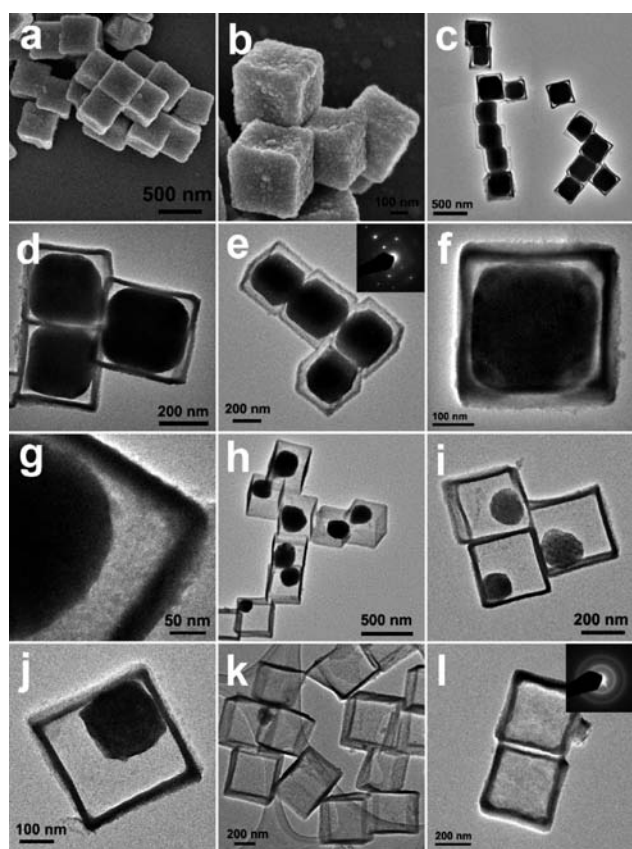


**Figure 3.** SEM and TEM images of hollow structures synthesized by templating against  $\text{Cu}_2\text{O}$  nanocubes: (a–g)  $\text{Cu}_2\text{O}@Fe(\text{OH})_x$  nanorattles obtained after immediate reaction; (h–j)  $\text{Cu}_2\text{O}@Fe(\text{OH})_x$  nanorattles obtained after reaction for 10 min; (k and l)  $Fe(\text{OH})_x$  nanoboxes obtained after reaction for 20–30 min.

No signals from possible impurities such as  $\text{Cu}(\text{OH})_2$  are detected in both samples of nanorattles and nanoboxes.

Figure 3a–g shows scanning electron microscopy (SEM) and transmission electron microscopy (TEM) images of cubic nanorattles synthesized after immediate reaction between  $\text{Cu}_2\text{O}$  nanocubes and  $Fe(\text{III})$  ions. The nanorattles well inherit the uniform size and shape of  $\text{Cu}_2\text{O}$  templates, of which the core size is around 300–350 nm in edge length and the shell is as thin as about 10–20 nm. Despite of the short period of precipitation, the iron hydroxide shells well duplicate the cubic

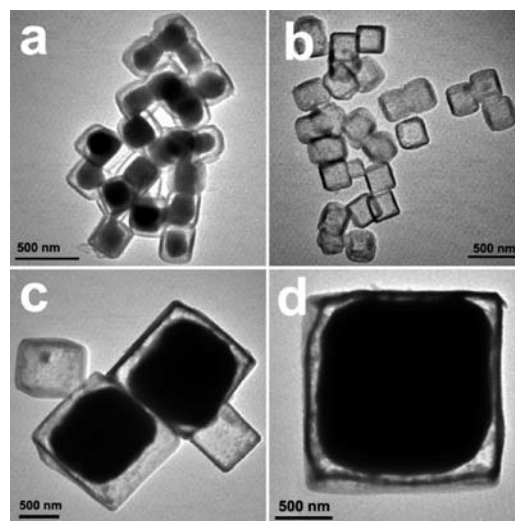


**Figure 4.** TEM images of (a)  $\text{Cu}_2\text{O}@Fe(\text{OH})_x$  nanorattles and (b)  $Fe(\text{OH})_x$  nanoboxes synthesized by templating against small  $\text{Cu}_2\text{O}$  nanocubes (200–250 nm); (c and d) nanorattles synthesized by templating against large  $\text{Cu}_2\text{O}$  cubes ( $\sim 1.5 \mu\text{m}$ ).

morphology of  $\text{Cu}_2\text{O}$  templates and are relatively smooth without openings on the surface. It is observed that in most cases the  $\text{Cu}_2\text{O}$  cores inside the shells are truncated cubes in shape. The etching should start from corner sites where the reactivity is enhanced as a result of sharp surface curvature. With continuous etching for a longer time such as 10 min, the  $\text{Cu}_2\text{O}$  cores evolve to be spherical in shape with the size significantly reduced, as shown in Figure 3h–j. Eventually, hollow nanoboxes of iron hydroxides are produced after complete dissolution of solid  $\text{Cu}_2\text{O}$  templates in 20–30 min (Figure 3k,l). The selected area electron diffraction (SAED) analysis indicates that these nanoboxes are nearly amorphous in nature, consistent with the above XRD results. Throughout the dissolution of  $\text{Cu}_2\text{O}$  crystals, there is no visible variation in the morphology of iron hydroxide shells, implying a much faster etching rate of  $\text{Cu}_2\text{O}$  templates than that for shell construction. It is further noted that continuous dissolution of  $\text{Cu}_2\text{O}$  can occur rapidly even in closed shells. This proves once again that species can quite freely transport across the shells during the etching process. In addition, the size of hollow structures can be easily modulated by templating against  $\text{Cu}_2\text{O}$  templates with different dimensions. Figure 4 shows TEM images of nanorattles and nanoboxes with two sizes of around 200–250 nm and over 1.5  $\mu\text{m}$ , which are fabricated through etching against  $\text{Cu}_2\text{O}$  nanocubes of respective sizes. With smaller  $\text{Cu}_2\text{O}$  nanocubes as templates, hollow nanoboxes are obtained after reaction for only 10 min (Figure 4b). No structural degradation such as collapse or amalgamation occurs although the reaction proceeds much faster. When micro-sized  $\text{Cu}_2\text{O}$  cubes are used, the dissolution of the cores is quite slow, generating very small hollow interiors even after reaction for 1 h (Figure 4c,d).

The use of pregrown  $\text{Cu}_2\text{O}$  templates allows the shape and size of resultant hollow structures to be rationally designed. For example, well-defined octahedral rattles and hollow cages could be selectively synthesized by templating against  $\text{Cu}_2\text{O}$  octahedra bounded by eight {111} planes.<sup>69</sup> In this case, much higher concentrations (3–17 times the amount for making cubic

(69) Cao, Y. B.; Fan, J. M.; Bai, L. Y.; Yuan, F. L.; Chen, Y. F. *Cryst. Growth Des.* **2010**, *10*, 232.

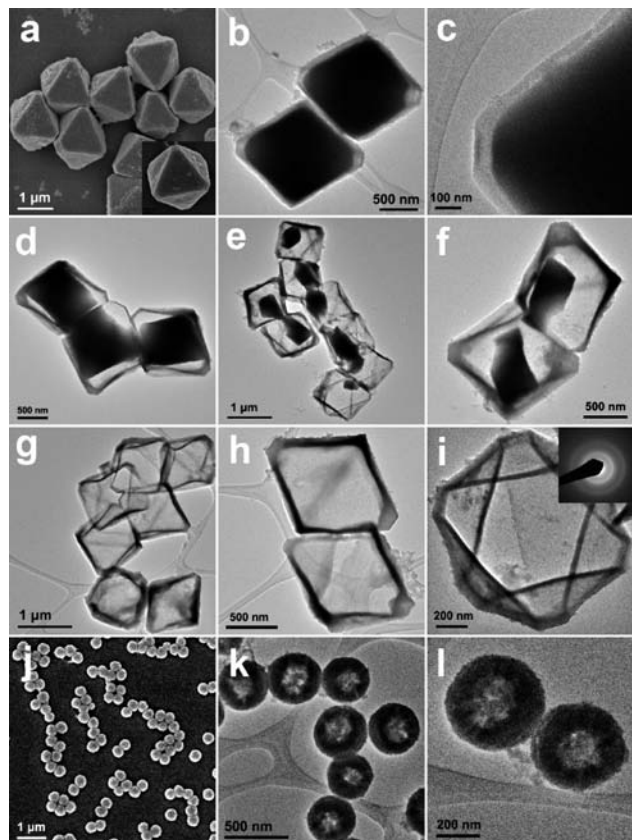


**Figure 5.** SEM and TEM image of hollow structures with different morphologies: (a–c) octahedral  $\text{Cu}_2\text{O}/\text{Fe}(\text{OH})_x$  core–shell structures; (d) and (e and f) octahedral rattles made by reacting with  $\text{Fe}(\text{III})$  ions with a higher concentration for 1 h and 3 h, respectively; (g–i) octahedral cages of iron hydroxides obtained after reaction for 4 h; (j–l) hollow spheres of iron hydroxides obtained after reaction for 10–20 min.

products) of  $\text{Fe}(\text{III})$  ions and a longer reaction time are required for efficient etching of  $\text{Cu}_2\text{O}$  octahedra due to their large size and the dominance of stable  $\{111\}$  surfaces with the lowest surface energy.<sup>69</sup> When etching by  $\text{Fe}(\text{III})$  ions with relatively lower concentrations (27.75–55.49 mM),  $\text{Cu}_2\text{O}/\text{Fe}(\text{OH})_x$  core–shell structures are made after reaction for 1 h, as shown in Figure 5a–c. This process can be significantly accelerated by increasing the concentration of  $\text{Fe}(\text{III})$  ions to 92.5 mM. The octahedral  $\text{Cu}_2\text{O}/\text{Fe}(\text{OH})_x$  rattles start to form after reaction for 30 min with continuous shrinkage of the  $\text{Cu}_2\text{O}$  cores in the course of 3 h of treatment (Figure 5d–f). After reaction for 4 h, octahedral cages of iron hydroxides are eventually obtained after complete dissolution of  $\text{Cu}_2\text{O}$  cores, as can be seen in Figure 5g–i. Same as cubic  $\text{Fe}(\text{OH})_x$  nanoboxes, the octahedral cages also possess smooth thin shells with amorphous texture indicated by SAED analysis (Figure 5i, inset). When the redox etching reaction is exploited against polycrystalline  $\text{Cu}_2\text{O}$  nanospheres, uniform hollow spheres are produced under properly controlled conditions, although the shell quality is not as good as that of the ones obtained from single crystal  $\text{Cu}_2\text{O}$  templates (Figure 5j–l).

The multicomponent characteristic of rattle-like structures enables their compositions to be tailored at different structural levels, which further generates a broad family of novel structures with hollow interiors. By carefully controlling the annealing conditions, rattles and cages with various shapes, dimensions, and compositions could be further derived. During the annealing process, iron hydroxide shells are found robust enough

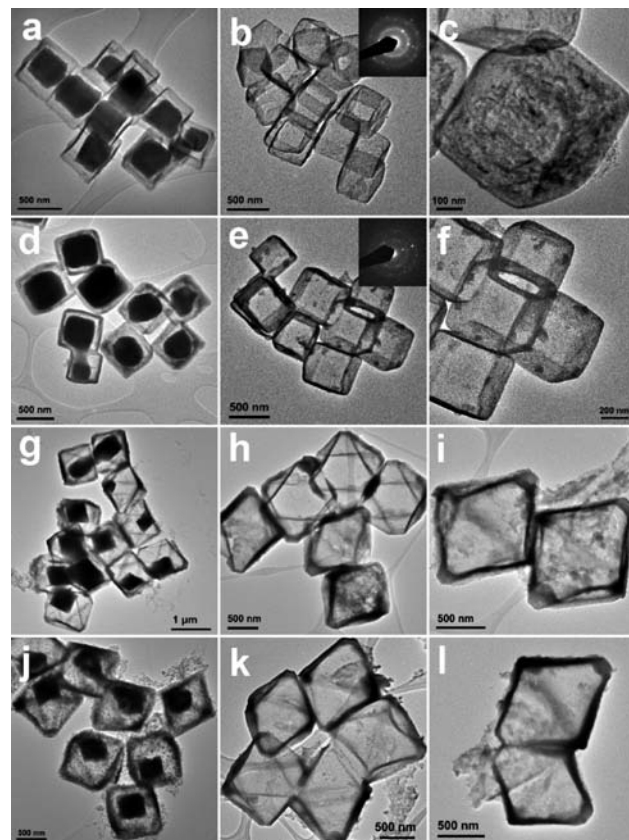


**Figure 6.** TEM images of the products after annealing under different conditions: (a)  $\text{Cu}_2\text{O}/\text{Fe}_2\text{O}_3$  nanorattles; (b and c)  $\alpha\text{-Fe}_2\text{O}_3$  nanoboxes; (d)  $\text{Cu}/\text{Fe}_3\text{O}_4$  nanorattles; (e and f)  $\text{Fe}_3\text{O}_4$  nanoboxes; (g) octahedral  $\text{Cu}_2\text{O}/\text{Fe}_2\text{O}_3$  rattles; (h and i) octahedral  $\alpha\text{-Fe}_2\text{O}_3$  cages; (j) octahedral  $\text{Cu}/\text{Fe}_3\text{O}_4$  rattles; (k and l) octahedral  $\text{Fe}_3\text{O}_4$  cages.

to withstand heat treatment upon converting to iron oxides at 250 °C despite of their thin shells and amorphous texture. Figure 6a–c displays TEM images of the products obtained by annealing cubic  $\text{Cu}_2\text{O}/\text{Fe}(\text{OH})_x$  nanorattles and  $\text{Fe}(\text{OH})_x$  nanoboxes in air. XRD analysis (Supporting Information Figure S1a) indicates the formation of  $\alpha\text{-Fe}_2\text{O}_3$  phase (as shells) while the  $\text{Cu}_2\text{O}$  phase (as cores) remains intact. Therefore, the products obtained are well-defined  $\text{Cu}_2\text{O}/\text{Fe}_2\text{O}_3$  nanorattles and  $\alpha\text{-Fe}_2\text{O}_3$  nanoboxes with a polycrystalline nature (Figure 6b, inset). When annealed in a  $\text{H}_2/\text{N}_2$  flow, XRD examination (Figure S1b) shows that  $\text{Cu}_2\text{O}/\text{Fe}(\text{OH})_x$  nanorattles have been reduced to polycrystalline  $\text{Cu}/\text{Fe}_3\text{O}_4$  nanorattles (Figure 6d). Such a hybrid structure characterized by confining metal nanocrystals inside magnetic shells may be very appealing as magnetically recyclable catalyst. By a similar procedure, magnetic  $\text{Fe}_3\text{O}_4$  nanoboxes with a polycrystalline nature (Figure 6e, inset) are also fabricated from  $\text{Fe}(\text{OH})_x$  nanoboxes, as shown in Figure 6e,f. When the same protocols are employed on hollow structures with other shapes, products with similar compositions could also be fabricated, as demonstrated by octahedral  $\text{Cu}_2\text{O}/\text{Fe}_2\text{O}_3$  and  $\text{Cu}/\text{Fe}_3\text{O}_4$  rattles, as well as  $\text{Fe}_2\text{O}_3$  and  $\text{Fe}_3\text{O}_4$  cages (Figure 6g–l).

During the formation of above hollow structures, the  $\text{Fe}(\text{OH})_x$  layer is deposited on the interface between solid  $\text{Cu}_2\text{O}$  and the bulk solution containing iron ions through the simultaneous redox etching and hydrolysis reaction. The formed shells are very thin and amorphous in texture, allowing efficient mass diffusion across them. This feature not only enables fast dissolution of  $\text{Cu}_2\text{O}$  templates within closed shells, but also

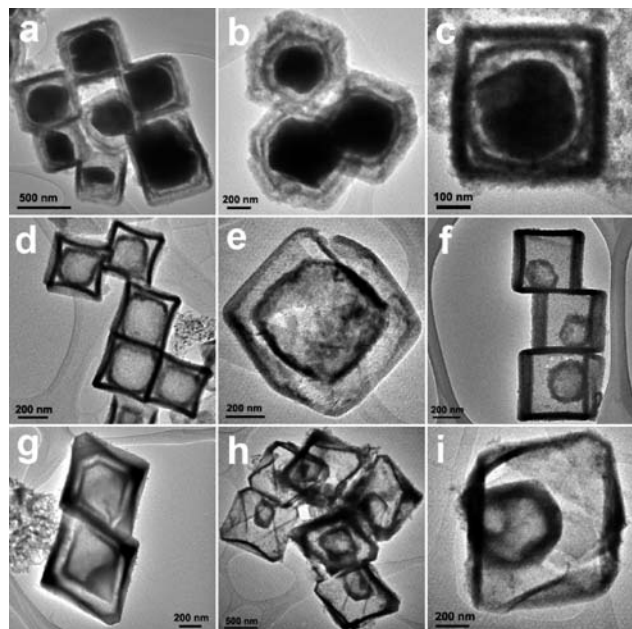


**Figure 7.** TEM images of hollow structures with complex interiors: (a–c) cubic double-walled  $\text{Cu}_2\text{O}@Fe(\text{OH})_x$  nanorattles; (d–f)  $Fe(\text{OH})_x$  box-in-box structures containing inner boxes with different sizes; (g–i) octahedral box-in-box  $Fe(\text{OH})_x$  cages.

offers the possibility of subsequent creation of inner shells in a top-down manner by chemical manipulation of preformed nanorattles, as schematically illustrated in Figure 1. In principle, such a procedure for making multishelled hollow structures is quite different from conventional bottom-up strategies where the inner shell is always formed before the outer shell.<sup>8,19,34,37,14,55–57</sup> Experimentally, this concept is demonstrated by template-engaged redox etching of the  $\text{Cu}_2\text{O}$  cores inside cubic  $Fe(\text{OH})_x$  nanoboxes with  $Fe(\text{III})$  ions under similar conditions for making single-shelled hollow structures. Smaller nanorattles or nanoboxes can be formed inside preformed  $Fe(\text{OH})_x$  “nanoreactors”, resulting in double-walled hollow structures with complex interiors, as shown in Figure 7. In such structures, both dimension and morphology of inner shells can also be tailored, depending on the configuration of  $\text{Cu}_2\text{O}$  cores in preformed  $Fe(\text{OH})_x$  nanoreactors. For instance, with  $\text{Cu}_2\text{O}@Fe(\text{OH})_x$  nanorattles obtained after immediate reaction as templates, double-walled nanorattles and nanoboxes with a nearly cubic inner shell can be synthesized by reacting with  $Fe(\text{III})$  ions for a very short time or for 20–30 min, respectively (Figure 7a–e). When  $\text{Cu}_2\text{O}@Fe(\text{OH})_x$  nanorattles made after reaction for 10 min are used as the starting material, hollow structures with a smaller spherical inner ball are produced after complete etching of the  $\text{Cu}_2\text{O}$  cores, as shown in Figure 7f. By a similar top-down strategy, double-shelled octahedral hollow structures can also be obtained (Figure 7g–i).

It should be pointed out that, in the present strategy, precise control on the hydrolysis of  $Fe(\text{II})/Fe(\text{III})$  ions is crucial for producing high-quality hollow structures. Excessively fast hydrolysis not only causes inevitable formation of abundant irregular impurities in solution, but also dramatically accelerates the redox etching by decreasing the pH value of the solution (see eq 1), which might further induce severe collapse of hollow structures upon rapid mass transport across the shells. One way to circumvent this problem is to introduce proper amount of nonaqueous solvent such as ethanol into the reaction system. This will slow down the hydrolysis of

$Fe(\text{II})/Fe(\text{III})$  ions so that nanoscale deposition can occur preferentially along the accessible surfaces of templates. In this work, the volume ratio between ethanol and water is optimized to be 49:1 to ensure both precipitation of iron hydroxides and redox etching of  $\text{Cu}_2\text{O}$  to take place at appropriate rates. A lower ethanol–water ratio, for example 40:10, causes collapse of hollow structures and generation of large quantities of impurities, as shown in Figure S2a,b. On the other hand, in the absence of water, hollow structures are hardly formed because hydrolysis of  $Fe(\text{II})/Fe(\text{III})$  ions does not occur in pure ethanol (Figure S2c,d). In addition, one drawback of ethanol-rich systems is the decreased ionizability of the mixed solvent, which significantly inhibits the etching of  $\text{Cu}_2\text{O}$  templates owing to lack of sufficient  $Fe(\text{III})$  ions in solution. Hence, strong inorganic electrolytes such as  $\text{NaCl}$  are introduced to improve the ionic strength of the solution. To verify the role of  $\text{NaCl}$  in the growth of hollow structures, experiments with the same mole concentration of other inorganic electrolytes such as  $\text{KCl}$  and  $\text{NaNO}_3$  are conducted under similar conditions, of which the results are shown in Figure S3. In the presence of these two salts, hollow structures, including both nanorattles and nanoboxes, could also be made following the same route despite of the slight difference in quality. However, without introduced electrolytes, hollow structures cannot form due to a quite slow etching rate. In brief, the presence of proper electrolyte in ethanol-rich solution offers an appropriate ionic environment for redox etching of  $\text{Cu}_2\text{O}$  crystals by  $Fe(\text{III})$  ions, but without the risk arising from fast hydrolysis in aqueous solution. As a result, hollow structures with well-defined shell structure and desirable complexity of the interiors are only produced under optimized conditions by utilizing the interplay and synergy of redox etching and hydrolysis reaction.

The synthetic strategy presented here provides a very facile route for preparing hollow structures, especially those with nonspherical shapes, by template-engaged redox etching of shaped  $\text{Cu}_2\text{O}$  crystals. In general, any metal salts capable of oxidizing  $\text{Cu}_2\text{O}$  can serve as potential precursors for shell construction, and the etchants for interior creation. Here, the versatility of this concept is demonstrated by successful synthesis of  $\text{Au}$  and  $\text{MnO}_x$  based hollow structures with various shapes. By replacing  $FeCl_3$  with  $\text{HAuCl}_4$  (reduction potential: 0.99 V for  $\text{AuCl}_4^-/\text{Au}$  pair), a variety of products, including  $\text{Cu}_2\text{O}@Au$  core/shell structures and cubic nanorattles and  $\text{Au}$  nanoboxes, are successfully synthesized following a similar route for making  $Fe$ -based hollow structures (Figure S4). Unlike those synthesized in boiling solutions, the surface of  $\text{Au}$  shells made here are polycrystalline and quite rough in texture, possibly due to the absence of crystal reconstruction processes, such as Ostwald ripening, at room temperature.<sup>32,50,70</sup> Similarly, well-defined  $\text{Cu}_2\text{O}@MnO_x$  nanorattles can also be fabricated by etching  $\text{Cu}_2\text{O}$  crystals in acidic solution of  $\text{KMnO}_4$ , as shown in Figure S5.

## Conclusions

We have demonstrated a facile strategy for synthesis of  $Fe(\text{OH})_x$  hollow structures with designed shapes and complex interiors by template-engaged redox etching of shape-controlled  $\text{Cu}_2\text{O}$  crystals. This method allows the morphology and dimension of resultant products to be rationally tailored,

(70) Roosen, A. R.; Carter, W. C. *Phys. A* **1998**, *261*, 232.

forming a variety of uniform hollow structures such as  $\text{Cu}_2\text{O}@\text{Fe}(\text{OH})_x$  nanorattles with tunable core size and  $\text{Fe}(\text{OH})_x$  cages. The interplay and synergy of redox etching and hydrolysis reaction between  $\text{Cu}_2\text{O}$  and  $\text{Fe}(\text{III})$  ions are responsible for formation of well-defined hollow architectures with desirable interiors. The multicomponent characteristic of rattle-like structures also enables one to modulate their composition at different structural levels, which further generates a broad family of interesting structures such as  $\text{Cu}_2\text{O}@\text{Fe}_2\text{O}_3$  and  $\text{Cu}@\text{Fe}_3\text{O}_4$  rattles, as well as  $\text{Fe}_2\text{O}_3$  and  $\text{Fe}_3\text{O}_4$  cages with various shapes.

The interiors of these  $\text{Fe}(\text{OH})_x$  hollow structures are highly accessible to reaction species. This feature offers the possibility of manipulation of the interior architecture inside preformed nanoscale reactors. The concept is demonstrated by successful preparation of double-walled nanorattles and box-in-box structures by template-engaged redox etching of the  $\text{Cu}_2\text{O}$  core inside the  $\text{Fe}(\text{OH})_x$  shell. Such a top-down approach for making

multishelled hollow structures is conceptually very different from conventional bottom-up strategies. Our preliminary results show that complex hollow structures for Au and  $\text{MnO}_x$  can also be obtained by this strategy. We believe that the concepts demonstrated in this work should be general, and will shed some light on fabrication of hollow structures with engineered interiors.

**Acknowledgment.** The authors are grateful to the reviewers for their valuable comments. X. W. Lou is grateful to the Nanyang Technological University and Ministry of Education (Singapore) for financial support through the start-up grant (SUG) and AcRF Tier-1 funding (RG 63/08, M52120096), respectively.

**Supporting Information Available:** XRD patterns; more TEM and SEM images. This material is available free of charge via the Internet at <http://pubs.acs.org>.

JA107871R